

Deposition of ZnO thin films on Si by RF magnetron sputtering with various substrate temperatures

Deok-Kyu Kim · Choon-Bae Park

Received: 6 June 2014 / Accepted: 12 September 2014 / Published online: 23 September 2014
© Springer Science+Business Media New York 2014

Abstract Undoped ZnO thin films were successfully deposited on Si substrates by RF magnetron sputtering with different substrate temperatures. The dependence was systematically investigated the structural, morphology, chemical state and optical properties of ZnO thin films. Crystal quality, growth orientation and optical properties of ZnO thin films were improved at proper substrate temperature (450 °C) whereas were deteriorated at higher temperature (600 °C). X-ray photoelectron spectroscopy showed that proper substrate temperature promoted the formation of Zn–O bonding, resulting in an improvement of film quality, while higher temperature decreased the formation of the Zn–O bonding and increased the oxygen vacancy due to formation of an amorphous SiO₂ layer at the interface of ZnO and Si, resulting in a degradation of film quality. Moreover, the amorphous SiO₂ layer is formed by oxygen related to the Zn–O bonding, mainly. Therefore, the experimental results indicate that the substrate temperature plays an important role in the deposition of ZnO film on Si substrate and needs to be carefully selected to suppress a formation of an amorphous SiO₂ layer.

1 Introduction

Recently, ZnO, a II–VI type compound semiconductor, has been a popular application material for optical devices

such as light emitting diodes (LED) and ultraviolet (UV) detector in the ranges of short wave [1, 2]. ZnO has a band gap of 3.37 eV in a direct transition in room temperature and a high optical transmittance for lights from infrared (IR) to visible range. Also, ZnO has a similar property as GaN using a blue LED material, and has higher exciton binding energy (60 meV) than that of GaN (25 meV), so that it is expected to show a superior property than GaN when the optical device in wide bandgap range was fabricated [3]. Si has been widely used in the electronics industry for a variety of well-developed technologies. It certainly has a lot of advantages if high quality ZnO thin films could be grown on a bare Si substrate. However, the growth of high quality ZnO films directly on Si substrates is difficult and often results in amorphous or polycrystalline films because of the large lattice mismatch between Si and ZnO and the formation of an amorphous SiO₂ layer at the interface of ZnO and Si [4, 5]. Nevertheless, ZnO thin films grown on Si substrates are very important for improving the efficiencies of optoelectronic devices fabricated utilizing ZnO/Si heterostructures. In addition, the successful growth of ZnO thin films on Si substrates requires better understanding of the mechanical characteristics in addition to its optical and electrical performances. However, there have been only a few studies on the systematical effect of the sputtering parameters, such as the substrate temperature, annealing temperature, sputtering power and ratio of oxygen to argon gas flow, on the various properties of ZnO thin films on Si substrates in detail [6, 7]. In this study, ZnO thin films were deposited on Si substrate by RF sputtering method with various substrate temperatures. We investigated the effects of substrate temperature on the structural, morphology, chemical bonding and optical properties of ZnO thin films.

D.-K. Kim
Advanced Development Team, Samsung Electronics Co. Ltd.,
Yongin, Gyeonggi 446-711, Korea

C.-B. Park (✉)
Department of Information and Communication Engineering,
Wonkwang University, Iksan, Jeonbuk 570-749, Korea
e-mail: cbpark@wonkwang.ac.kr

2 Experimental procedure

ZnO thin films of ~200-nm thickness were deposited on Si (111) substrates by RF magnetron sputtering at various deposition temperatures. Before the deposition, the substrates were ultrasonically cleaned with acetone and alcohol in sequence for 5 min, then dipped into the buffered HF (HF: deionized water = 7:1) to remove a native oxide layer on them, and finally rinsed with deionized water and dried in nitrogen. The base pressure in the chamber was 8.0×10^{-6} Torr by a turbomolecular pump, and the working pressure was 15 mTorr. The ZnO target (99.999 % purity) was etched by sputtering for 10 min in argon and oxygen ambient to clean its surface. Films deposition was made using argon and oxygen plasma at 40 sccm and 10 sccm, respectively, and RF power of 120 W. The deposition temperature was set to 300, 450, and 600 °C. After depositing the ZnO films, thin films were post-annealed in same chamber using in situ method. The ZnO thin films were annealed for 20 min in O₂ atmosphere at 400 °C. After heat treatment, natural cooling was performed.

The structural characteristics of the sample were analyzed by X-ray diffraction (XRD, D/MAXIII A) using Cu K α line (1.54055 Å). The surface textures of the samples were observed by scanning electron microscopy (SEM, JSM-6400). For chemical analysis, X-ray photoelectron spectroscopy (XPS, EscaLab 250, VG Scientific) measurements with Al K α radiation (1,486.6 eV) were carried out and were calibrated with C 1s peak (284.6 eV). Optical transmittance was determined using UV/VIS/NIR spectrophotometer (SHIMADZU, UV-2401PC) in the spectral range of 300–700 nm.

3 Results and discussions

Figures 1 and 2 show the XRD results of ZnO thin films deposited at various substrate temperatures. All ZnO thin films have a strong (002) diffraction peak and a weak (103) diffraction peak, regardless of the substrate temperature (not shown here). This indicates that the ZnO thin films are polycrystalline, with hexagonal crystals, and have a well-defined c-axis orientation perpendicular to the substrate. The (002) plane of a ZnO thin film is the most thermodynamically favorable growth plane because of its low surface energy and the most densely packed in the wurtzite structure. As substrate temperature increases, the intensity of the (002) peak increases and then decreases, whereas the intensity of the (103) peak increases linearly. To quantitatively investigate the degree of preferred orientation of the ZnO thin films, the texture coefficients (TC) of (002) planes are calculated by following formula [8]:

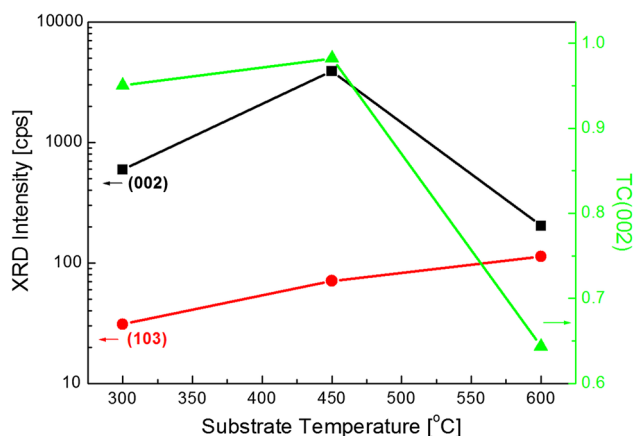


Fig. 1 XRD peak intensities from (002) and (103) planes and TC(002) of ZnO thin films deposited at various substrate temperatures

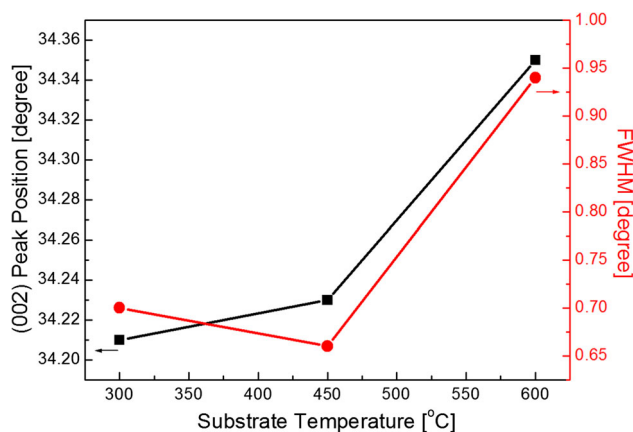


Fig. 2 (002) peak position and FWHM of ZnO thin films deposited at various substrate temperatures

$$TC(hkl) = \frac{I(hkl)}{\sum I(hkl)} \times 100\%$$

where $TC(hkl)$ is the texture coefficient of (hkl) plane, $I(hkl)$ is the intensity of the (hkl) plane. When the substrate temperature increases, the value of TC of (002) planes increases and then decreases, drastically. At the substrate temperature of 450 °C, the improvement of the (002) preferred crystallographic orientation is ascribed to the surface diffusion of the adsorbed atoms increasing, inducing an improvement of the crystallinity [9]. Whereas, the degradation of the (002) preferred orientation at 600 °C can be explained by the change in the surface energy of ZnO crystal due to the formation of an amorphous SiO₂ layer at the interface of ZnO and Si [10]. That is, an amorphous SiO₂ layer formed at 600 °C leads to reduce the intensity of the (002) peak and increase the intensity of the (103) peak, resulting in decrease of the (002) preferred orientation.

The (002) peak positions for ZnO thin films prepared at 300, 450, and 600 °C appear at 34.21°, 34.23°, and 34.35°, respectively. Compared with the (002) peak position of bulk ZnO (34.42°), the diffraction angle of ZnO thin films decreases, which results in the increase of interplanar spacing. This indicates that all ZnO films suffer compressive stress. Generally, since the thermal expansion coefficient of ZnO along an axis ($6.5 \times 10^{-6} \text{ }^\circ\text{C}^{-1}$) was higher than that of Si ($3.59 \times 10^{-6} \text{ }^\circ\text{C}^{-1}$), tensile stress would be generated when the substrate temperature dropped from high temperature down to RT. In our experiment, the compressive stress exists in films deposited at an all substrate temperature, which indicates that the compressive stress originates from the intrinsic stress due to the defects in the ZnO lattice rather than the thermal stress [11, 12]. It is well known that zinc interstitials or oxygen vacancies are easily formed in ZnO, and they will induce the compressive or tensile stress. As the substrate temperature increases, the diffraction angles of ZnO thin films increase, which indicates that c-axis values of ZnO films are shortened, and thus the compressive stress in these ZnO films becomes relaxation because of tensile stress along the interfaces originating from the thermal stress. We confirmed that the stress changing in the film is due to intrinsic stress related to the defects in the ZnO lattice and the thermal stress with increasing substrate temperature. That is, the predominant factor influencing the film stress under low substrate temperature is intrinsic stress related to the defects in the ZnO lattice, while the thermal stress becomes more important as the substrate temperature increases.

With an increase in the substrate temperature, the full width at half maximum (FWHM) for ZnO thin films decreased and then increased; 0.7° at 300 °C, 0.66° at 450 °C and 0.94° at 600 °C. As mentioned above, the improvement of crystallinity at 450 °C and the degradation at 600 °C is attributed to the migration of the deposition atoms and the formation of amorphous SiO₂ layer at interface, respectively [9, 10]. The average crystallite sizes of the films were calculated using the Scherrer equation [13]:

$$D = \frac{0.9\lambda}{B \cos \theta}$$

where λ is the wavelength of X-ray radiation (1.5406 Å), B is the FWHM of the sample, and θ is the Bragg diffraction angle. The average crystallite size increases from 11.9 nm to 12.6 nm and then decreases to 8.8 nm with an increase in the substrate temperature. From the XRD results, it can be concluded that a proper substrate temperature can greatly improve the crystalline quality of ZnO thin films. Also, these results are in good agreement with those reported earlier in literature [14].

Figure 3 shows the SEM images of ZnO thin films deposited at different substrate temperatures. The

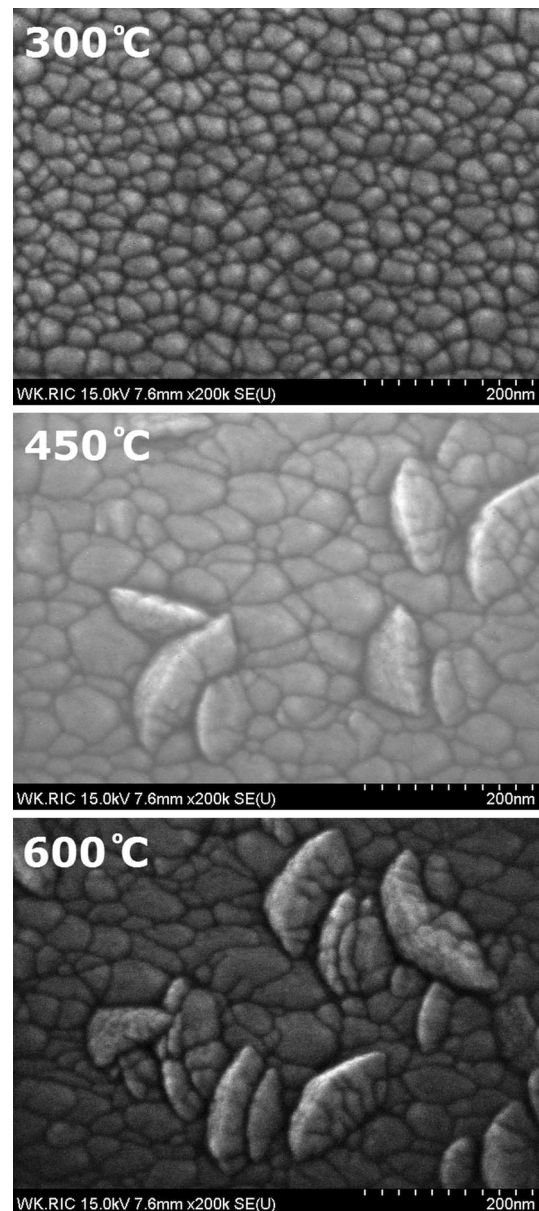


Fig. 3 SEM images of ZnO thin films as function of substrate temperatures

morphology of ZnO thin film deposited at 300 °C is uniform consisting of homogeneous and densely packed distribution of quite small round-shape grains, which is the traditional morphology in thin films with c-axis preferred orientation. As the substrate temperature increases to 450 °C, the round-shape grain size evidently become larger than sample of 300 °C and there occurs lenticular-shape grains. With the substrate temperature increasing to 600 °C, the round-shape grain size is constant but there are more lenticular-shape grains than sample of 450 °C. The grain size observed from SEM images and XRD results is listed in Table 1. From Table 1, the average grain size

Table 1 Average grain size and ratio of ZnO thin films deposited at various substrate temperatures

Substrate temperature (°C)	Gs (nm) (grain size by SEM)	Gx (nm) (grain size by XRD)	Ratio (Gs/Gx)
300	30	11.9	2.52
450	60	12.6	4.76
600	60	8.8	6.82

obtained by the SEM observation is different from that found by XRD method. It is believed that the former may reflect the mean grain size in the lateral direction and the latter, the size in the height direction. The ratio of average grain size in the lateral direction to that in height direction increases with increasing substrate temperature, as seen from Table 1. At 300 °C, the average grain size in the lateral direction is 2.52 times larger than that in the height direction. As the substrate temperature increases to 450 and 600 °C, the grain size in the lateral direction is much larger than that in height direction. This might due to the fact that the sputtered atoms gain enough energy for migration on any direction at higher temperature. Also, the change in surface structure, the formation of lenticular-shape grains, is thought to correspond to the change in crystal orientation as the XRD results. Namely, the lenticular-shape grains seems to originate from (103) preferred orientation, which is due to an amorphous SiO₂ at the interface of ZnO and Si [15, 16]. We presume that the evolution of microstructure would be powerfully related to the migration of atoms and the formation of an amorphous SiO₂ during the deposition.

In order to analyze the origin of the variation in structural properties of the ZnO thin films deposited at various substrate temperatures, the chemical bonding states were examined by XPS. All the samples were etched for 30 s to reduce the hydroxyl groups on their surfaces. The Zn 2p_{3/2} core level (1,021.2 ± 0.1 eV) spectra (not shown here), which correspond to the Zn–O bonds in ZnO film, is highly symmetric in shape, indicating that Zn existed only in their oxidized states [17]. The O 1s spectra showing the chemical bonding state of oxygen shows asymmetric peaks, as shown in Fig. 4. The O 1s spectra were deconvoluted into two peaks by two mixed 90 % Gaussian–10 % Lorentzian curves following the subtraction of the Shirley background. No peak related to surface hydroxyl groups is observed owing to the etching of the surfaces. The low binding energy (529.9 ± 0.1 eV) is associated with the O²⁻ ions of the wurtzite structure of the hexagonal Zn²⁺ ion array and these ions are surrounded by Zn atoms with their full complement of nearest-neighbor O ions [18]. The high binding energy (531.8 ± 0.1 eV) is corresponded to the O²⁻ ions present in the oxygen-deficient regions within the ZnO matrix [19]. Therefore, the relative changes in the

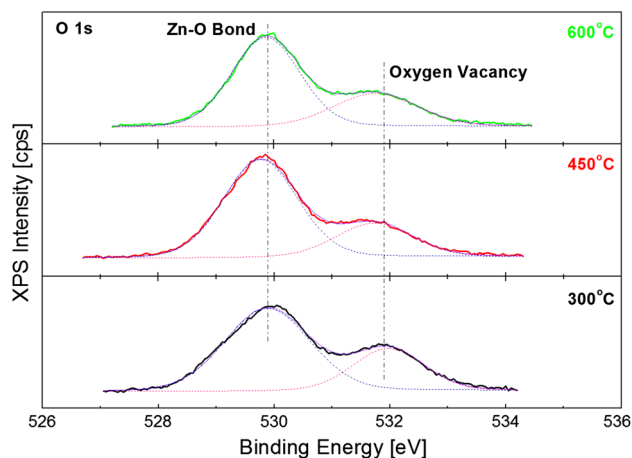


Fig. 4 XPS spectra for the O 1s states of ZnO thin films with different substrate temperatures

intensities of the low- and high-binding energy components may be related in part to the degree of Zn–O bonding and the number of oxygen vacancies available and are shown in Fig. 5. The increase in substrate temperature from 300 °C to 450 °C increases the peak area of the Zn–O bonding and decreases the peak area of the oxygen vacancy. This indicates that the increase in substrate temperature promoted the formation of the Zn–O bonding, whereas suppressed the formation of the oxygen vacancy together, resulting in improved crystalline quality. However, at a higher temperature of 600 °C, the peak area of Zn–O bonding decreases and the peak area of oxygen vacancy increases, suggesting that some of oxygen atoms might have been diffused and reacted with impurity atoms such as silicon from the silicon substrate [20]. Therefore, the crystalline quality at 600 °C is deteriorated by forming an amorphous SiO₂ layer at the interface of ZnO and Si. Also,

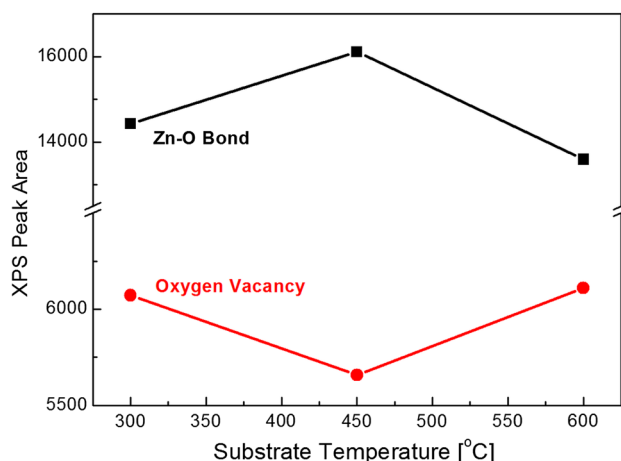


Fig. 5 Dependence of peak area for Zn–O bond and oxygen vacancy of ZnO thin films with different substrate temperatures

the peak area of oxygen vacancy at 600 °C is similar but the peak area of the Zn–O bonding is small, compared to 300 °C. This result shows that an amorphous SiO₂ layer is formed by oxygen related to the Zn–O bonding rather than that related to oxygen vacancy. The XPS results have good correlations to the changes in structural characteristics deduced from the XRD spectra in Fig. 2. As a result, the substrate temperature mainly determines the number of Zn–O bonds as well as the number of oxygen vacancies formed in the ZnO thin films. Especially, oxygen related to the Zn–O bonding contributes to form an amorphous SiO₂ layer, which lead to deteriorate the crystal quality of ZnO thin film. We conclude that a proper substrate temperature needs to deposit high quality ZnO thin films on Si substrate.

To obtain electrical properties of ZnO thin film, Hall measurement was carried out but couldn't be measured Hall measurement due to high resistance over M-ohm.

Figure 6 shows the optical transmittance of the ZnO films deposited at different substrate temperatures. The glass substrate was used to indirectly measure the optical transmittance because of opaque property of Si substrate. We confirmed a similar crystallinity change trend for ZnO films on Si and glass substrate in our pre-experiment. As seen in Fig. 6, all samples show a high transmittance in the visible region and a strong light absorption at around 380 nm, which correspond to the optical band gap of ZnO. The average transmittance in the visible range of 400–700 nm is found to vary from 84.2 to 89.3 %. The value of transmittance in visible region increases with increase to 450 °C which indicates that the ZnO films at 450 °C have less defects and better crystalline structure. It is well known that the optical transmittance of ZnO films depends

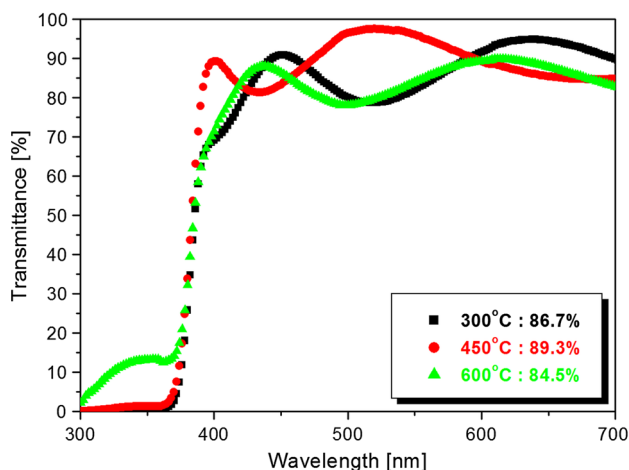


Fig. 6 Optical transmittance spectra of ZnO thin films prepared at various substrate temperatures

upon their crystalline structure [21]. We observe the highest optical transmittance of 89.3 % in the visible wavelength range for films deposited at 450 °C. The UV absorption edge firstly shifts to a shorter wavelength, which means that the optical band gap increases and it further shifts to a longer wavelength as substrate temperature increases to 600 °C. In order to calculate the optical band gap of the samples, the Tauc formula was used as follows [22]:

$$\alpha hv = A(hv - E_g)^n$$

where α is the optical absorption coefficient, A is the constant, hv is the photon energy, h is planck's constant, E_g is the optical band gap of sample. The constant n takes the value 1/2 for direct energy gap due to direct allowed transition for films which had polycrystalline structure and has the value 2 for indirect energy gap due to indirect allowed transition for films which has an amorphous structure. The relation between $(\alpha hv)^2$ and photon energy (hv) is shown in Fig. 7, in order to determine the direct optical energy gap for these films. The optical direct energy gap E_g can be calculated from the linear fitting curve between $(\alpha hv)^2$ and hv at $\alpha = 0$. The fitting results indicate that the optical band gap of ZnO films increases and then decreases with increase of substrate temperature, namely the absorption edge shifts toward shorter wavelength and then longer wavelength. It can be found that the optical band gap reaches a maximum of about 3.287 eV at 450 °C. We think the blue shift of the band gap may be mainly attributed to the high concentration of free electrons due to Burstein–Moss effect [23]. It is clear that the obtained energy gap depends mainly on the values of substrate temperature.

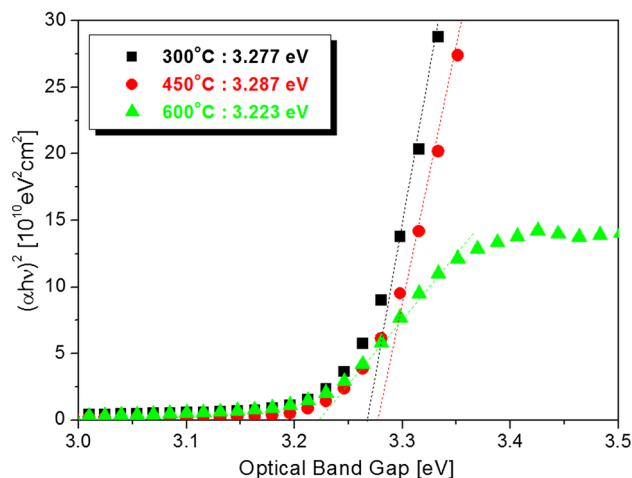


Fig. 7 $(\alpha hv)^2$ versus hv for AZO thin films prepared at various substrate temperatures

4 Conclusion

In this study, undoped ZnO thin films on Si substrate were prepared by RF magnetron sputtering with different substrate temperature and its properties were studied. The results showed that properties of ZnO thin films were significantly affected by the substrate temperature. The improvement at proper substrate temperature (450 °C) was attributed to promote Zn–O bonding, resulting in improved film quality, whereas the deterioration at higher temperature was ascribed to form an amorphous SiO₂ layer at the interface of ZnO and Si. Therefore, the proper substrate temperature to hinder the formation of an amorphous SiO₂ layer is strongly needed for optoelectronic devices fabricated utilizing ZnO/Si heterostructures.

Acknowledgments This paper was supported by Wonkwang University in 2014.

References

1. S.L. Ou, D.S. Wu, S.P. Liu, Y.C. Fu, S.C. Huang, R.H. Horng, *Opt. Express* **19**, 16244 (2011)
2. H.H. Li, P.Y. Yang, S.M. Chiou, H.W. Liu, H.C. Cheng, *IEEE Electron Device Lett.* **32**, 928 (2011)
3. X. Zou, G. Fang, J. Wan, N. Liu, H. Long, H. Wang, X.Z. Zhao, *Semicond. Sci. Technol.* **26**, 055003 (2011)
4. Y.Y. Chen, J.R. Yanga, S.L. Cheng, M. Shiojiri, *Thin Solid Films* **545**, 183 (2013)
5. M. Jung, J. Lee, S. Park, H. Kim, J. Chang, *J. Cryst. Growth* **283**, 384 (2005)
6. H. Chen, J. Ding, W. Guo, *Ceram. Int.* **40**, 4847 (2014)
7. J.J. Ding, H.X. Chen, S.Y. Ma, *Physica E* **42**, 1861 (2010)
8. J. Zhai, L. Zhang, X. Yao, *Ceram. Int.* **26**, 883 (2000)
9. Z. Zhang, C. Bao, W. Yao, S. Ma, L. Zhang, S. Hou, *Superlattices Microstruct.* **49**, 644 (2011)
10. B. Houng, H.B. Chen, *Ceram. Int.* **38**, 801 (2012)
11. J. Mass, P. Bhattacharya, R.S. Katiyar, *Mater. Sci. Eng. B* **103**, 9 (2003)
12. R. Ondo-Ndong, G. Ferblantier, MAl Kalfioui, A. Boyer, A. Foucaran, *J. Cryst. Growth* **255**, 130 (2003)
13. B.D. Cullity, *Elements of X-ray Diffraction* (Addison-Wesley, Reading, 1978), p. 102
14. A.A. Lotin, O.A. Novodvorsky, D.A. Zuev, O.D. Khramova, L.S. Parshina, F.V. Lebedev, J.W. Bartha, C. Wenzel, *Opt. Mater.* **35**, 1564 (2013)
15. C.H. Ahn, S.Y. Lee, H.K. Cho, *Thin Solid Films* **545**, 106 (2013)
16. K. Maejima, T. Koida, H. Sai, T. Matsui, K. Sato, M. Kondo, T. Takagawa, *Thin Solid Films* **559**, 83 (2014)
17. C.D. Wagner, W.M. Riggs, L.E. Davis, J.F. Moulder, G.E. Muilenberg, *Handbook of X-ray Photoelectron Spectroscopy* (Eden Prairie, Mn, PerkinElmer Corporatio, 1979), pp. 50–51
18. V.I. Nefedov, M.N. Firsov, I.S. Shaplygin, *J. Electron Spectrosc. Relat. Phenom.* **26**, 65 (1982)
19. J.C. Fan, J.B. Goodenough, *J. Appl. Phys.* **48**, 3524 (1977)
20. S.-S. Lin, J.-L. Huang, P. Sajgalik, *Surf. Coat. Technol.* **190**, 39 (2005)
21. V. Senthilkumar, P. Vickraman, M. Jayachandran, C. Sanjeeviraja, *Vacuum* **84**, 864 (2010)
22. J. Tauc, *Mater. Res. Bull.* **5**, 721 (1970)
23. L. Burstein, *Phys. Rev.* **93**, 632 (1954)